

RSC Advances



This is an *Accepted Manuscript*, which has been through the Royal Society of Chemistry peer review process and has been accepted for publication.

Accepted Manuscripts are published online shortly after acceptance, before technical editing, formatting and proof reading. Using this free service, authors can make their results available to the community, in citable form, before we publish the edited article. This *Accepted Manuscript* will be replaced by the edited, formatted and paginated article as soon as this is available.

You can find more information about *Accepted Manuscripts* in the [Information for Authors](#).

Please note that technical editing may introduce minor changes to the text and/or graphics, which may alter content. The journal's standard [Terms & Conditions](#) and the [Ethical guidelines](#) still apply. In no event shall the Royal Society of Chemistry be held responsible for any errors or omissions in this *Accepted Manuscript* or any consequences arising from the use of any information it contains.

Cite this: DOI: 10.1039/c0xx00000x

www.rsc.org/xxxxxx

ARTICLE TYPE

Concentrated Synthesis of Metal Nanoparticles in Water

Rory Anderson¹, Richard Buscall², Robert Eldridge¹, Paul Mulvaney³, and Peter Scales^{1,*}¹Particulate Fluids Processing Centre, The Department of Chemical and Biomolecular Engineering, University of Melbourne, Victoria 3010, Australia²MSACT Research & Consulting, Exeter, EX2 8GP, United Kingdom³Bio21 Institute, University of Melbourne, Victoria 3010, Australia

*Corresponding Author. Email: peterjs@unimelb.edu.au

Received (in XXX, XXX) Xth XXXXXXXXX 20XX, Accepted Xth XXXXXXXXX 20XX

DOI: 10.1039/b000000x

The synthesis of a range of metal nanoparticles (Ag, Au, Pd, Pt) in water through reduction from the acid soluble salt at abnormally high concentrations (>1 mol/L) is demonstrated using a comb polymer of methoxypoly(ethylene glycol) acrylate and maleic anhydride (PEG-MA) as the particle stabiliser during particle formation. The results show that at high concentrations in water, the general growth mechanism in these systems is through aggregation of nuclei of an approximate diameter of 0.6 nm. Aggregation resulted in formation of single crystals up to a particle diameter of approximately 5 nm but thereafter, further aggregation resulted in polygonal twinned particles. Continued aggregation caused agglomerate particles to be formed at larger sizes (>30 nm). Stabiliser adsorption was found to be critical to size control whereby the aggregation process was interrupted, preventing further growth. A case of the synthesis of Ag nanoparticles with a mean size of 8nm at concentrations of up to 2.5 mol/L is elaborated.

Introduction

There is significant academic and industrial interest in nanoparticle synthesis since very small particles, particularly metals, exhibit a diverse range of novel properties with potential applications in areas such as agriculture, defence, health, electronics, the environment, and commerce¹. Despite the obvious potential, the wide scale application and adoption of nanoparticles into commodity products remains limited, largely because an economically viable and environmentally sustainable method of mass production for nanoparticles remains elusive. This is exemplified by the fact that it is preferred that synthesis be conducted at high concentrations, at a high rate and in an aqueous medium. Control of particle synthesis with these boundary conditions has proved difficult.

It is hypothesised that one reason for the difficulty experienced in the control of the synthetic route to nanoparticle nucleation and growth at high concentrations in water is that our understanding of these processes in the presence of an additive stabiliser are not well understood. The stabilising molecule needs to be capable of adsorbing rapidly as to prevent growth process, be an effective steric stabiliser, and adsorb strongly to overcome any displacement stresses that arise as a result of particle interactions. Nucleation in the absence of a stabiliser produces an aggregated amorphous mass of uncontrolled size.

Synthesis of nanoparticles is widely reported throughout the literature and there are many production methods that have been discussed both in organic solvents²⁻⁹ and in aqueous solution¹⁰⁻³⁶. Nanoparticles can be produced at high concentrations in

organic solvents and many workers report success using simple surfactants²⁻⁹. The primary disadvantage with using organic solvents as the synthetic media is that they present an ecological hazard and are thus not environmentally sustainable and many industries are moving away from such processes. Production in water mitigates the environmental concerns, yet results in a plethora of synthetic problems. It is not a case of simply changing the reaction medium and being able to continue producing nanoparticles at high concentration. Water is a highly polar molecule and therefore interacts with the stabiliser, potentially inhibiting its adsorption and stabilisation capabilities, leading to poor particle size control.

The difficulties associated with synthesis in aqueous systems are well known. Many research groups have focussed on comb structured polymers to aid nanoparticle stabilisation in water as opposed to surfactants or linear structured polymers^{13, 15, 26, 29, 30, 32, 33, 37}. The stabilisation efficacy of surfactants and linear polymers is limited in water. Physisorption is partially dependent on the contrast between the relative static permittivity (dielectric constant) between the solvent and the solid interface. Ionised head groups, which generally have high surface affinity due to the high surface energy of particles, are affected by the polarity of the solvent^{38, 39}. In non polar solvents, there is a large contrast and so the adsorption of the stabiliser to the particle surface is strong. However, in water the contrast is reduced and stabiliser adsorption is weaker. This makes stabiliser displacement from the particle surface more likely as steric layer stresses manifest themselves as stabilised particles interact⁴⁰. Not surprisingly therefore, it has been shown that the bonding strength of the adsorption units on the stabiliser is critically important^{13, 35, 41}. In

dilute systems, electrostatic repulsive forces offer a significant contribution to overall system stability, reducing steric layer stresses. However, at a high salt concentration, electrostatic repulsion becomes negligible and the van der Waals force between particles (attractive in this configuration) can only be negated by steric repulsive forces. Even then, there will always be the possibility of stabiliser displacement leading to particle aggregation.

The issue of weaker adsorption can be overcome through use of multiple adsorption groups. Chen *et al.* have demonstrated that stabilisers possessing multiple terminal bonding groups are more successful at adhering via physisorption to the particle surface, and that stabilisers containing a single terminal bonding group weakly adsorb¹³. Increasing the adsorption strength of the stabiliser helps to mitigate stabiliser displacement as a result of stresses that develop in the steric layer⁴². Increasing the number of adsorption groups can be achieved through use of a polymer. Linear polymers, such as poly acrylic acid (PAA), are often used. However, as with surfactants, linear polymers do not appear to be suitable for high concentration synthesis of nanoparticles in water. Steric repulsion is provided through loops and chain ends that form as the polymer adsorbs to the particle surface. An ideal stabiliser must be able to both strongly adsorb to the particle surface and have a component that extends away from the surface to provide steric repulsion^{43, 44}. In linear polymers at high salt, these requirements appear to be mutually exclusive. The problems inherent with both surfactants and linear polymers can be overcome through use of comb polymers. It has been found that copolymers are more effective in many instances at providing stabilisation than linear polymer analogues^{13, 26}. This is because the structure of a comb polymer allows strong surface adsorption, due to the presence of numerous adsorption groups along the backbone. Comb polymers also possess a component dedicated to providing steric stabilisation, which linear polymer analogues lack. This allows strong adsorption without compromising steric protection^{40, 42}.

While surfactants and linear polymers relying on physisorption are unlikely to be suitable as stabilisers at high concentrations, comb polymers are regarded as having potential^{13, 15, 26, 29, 32, 33, 37, 41}. Chen *et al.* found that a comb polymer of maleic anhydride with oligomeric oxyethylene side chain units was able to stabilise a Al_2O_3 -coated TiO_2 particle system far more effectively than the linear analogue, oligomeric oxyethylene units with terminal carboxyl groups¹³. Sidorov *et al.* conducted a comparison between a diblock and a comb copolymer composed of PEO and PEI. They found that the comb copolymer provided far more effective stabilisation²⁹. In both cases the superior performance of the comb polymer was attributed to the presence of a structural component dedicated to providing steric stabilisation^[12, 28].

This study involves the use of a comb polymer of methoxypoly(ethylene glycol) acrylate and maleic anhydride (PEG-MA) for use as a stabiliser in the synthesis of metal nanoparticles. PEG-MA is a comb polymer that has both a high density of adsorption groups and dedicated steric components. The maleic anhydride rings that form the backbone of the polymer undergo hydrolysis upon mixing with water. This results in the formation of two carboxyl groups for every maleic anhydride group. The high density of carboxyl groups aligning

the backbone of the stabiliser is expected to strongly anchor the stabiliser to the particle surface. The PEG component, which is highly soluble, is expected to extend into solution and provide a steric barrier.

It is proposed that this combination of a strong particle surface affinity and dedicated steric shielding should result in a PEG-MA comb polymer being an effective stabiliser for the synthesis of nanoparticles. Research conducted at Imperial Chemical Industries by Buscall *et al.* recognised a PEG-MA stabiliser as having potential for use in the stabilisation of nanoparticles in aqueous systems⁴⁵⁻⁴⁹. A range of particle dispersions, which predominately consisted of a narrow range of ionic compounds, were formed through precipitation of soluble precursor salts. However, particles of less than 100nm in diameter were not obtained. It was thought that optimisation of the structure of the PEG-MA comb polymer through different synthetic approaches would yield a successful candidate for use in the aqueous synthesis of highly concentrated nanoparticle suspensions.

The primary aim of this research was to develop a stabiliser that could be generally applied for use in the synthesis of stable metal nanoparticles at high concentrations in water. The particle systems chosen for analysis were: Ag, Au, Pd and Pt. These materials are all known to be non-reactive stable metals and therefore capable of forming viable and stable particles in aqueous systems. In order to understand the issues associated with nucleation and growth of metal nanoparticles in this concentrated dispersion, an evaluation of particle synthesis over a range of different conditions to assess the reaction kinetics and the formation mechanisms was conducted. Based on information obtained from these experiments, the Ag system was chosen to demonstrate that a PEG-MA comb polymer could be used to facilitate the high concentration synthesis of nanoparticles in water.

Experimental Methods

Materials

Ammonium hexachloropalladate(IV) ($(\text{NH}_4)_2\text{PdCl}_6$, 99.99%, Aldrich), hydrazine monohydrate ($\text{N}_2\text{H}_4 \cdot \text{H}_2\text{O}$, Sigma-Aldrich, 98%), ammonia solution ($\text{NH}_3(\text{aq})$, MERCK, 25wt%), silver nitrate (AgNO_3 , Fluka, $\geq 99.0\%$), gold (III) chloride (AuCl_3 , Aldrich, 99%), platinum (IV) chloride (PtCl_4 , Aldrich, $\geq 99.9\%$), hydrochloric acid (1M $\text{HCl}(\text{aq})$, Scharlau), and sodium borohydride (NaBH_4 , ICN Biomedicals Inc.) were used in the experimental preparation of nanoparticles. All chemicals were used as received, without further purification.

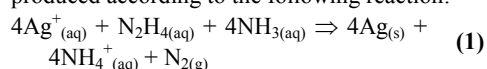
Polymer Synthesis

Short copolymers (telomers) of maleic anhydride and polyethyleneglycol acrylate (Aldrich, typical MW 454) were synthesised by heating the monomers (1.4:1 mol ratio) with 4,4'-azobis-4-cyanopentanoic acid (0.33 mol/mol PEG) in an acetone-DMF-toluene solution (2.4:1:10 w/w) for 4 hours at 90°. The dark red copolymers were precipitated in diethyl ether and washed 3 times with ether. After evaporation of residual ether the yield was typically 105% of the weight of PEG. The acid capacity, measured by titration with 0.1M KOH in 1M aqueous KCl, was typically 3.2mmol/g (c.f. calculated 3.6mmol/g for a 1:1 copolymer).

Synthesis of Concentrated Ag Nanoparticles

A semi-batch stirred tank reactor with a six-blade Rushton impeller was used in the synthesis of Ag nanoparticles according to the standard tank configuration as outlined by Holland and Chapman⁵⁰. All reactions were conducted at room temperature ($20 \pm 2^\circ\text{C}$).

The PEG-MA comb polymer was dissolved in water and a stoichiometric quantity of ammonia was added to deprotonate the polymer. Additional ammonia was added to prevent the formation of nitric acid as a by-product. Alternatively, ammonium nitrate is produced. At low pH hydrazine is unable to effectively reduce Ag^+ ⁵¹. AgNO_3 solution was then added and the total volume of solution in the reactor was brought to 80mL with deionised water. Hydrazine was then added to the reactor via a Harvard Apparatus PHD2000 infusion pump with a dosing rate of 10mL/hr for a total volume of 20mL. Ag particles were produced according to the following reaction:



During the reaction the vessel was mixed at a constant rate of 400 rpm. This provided an average velocity gradient for mixing of 150 s^{-1} . Once the synthetic reaction was complete, NO_3^- ions were removed from the system using a DOWEX® MONOSPHERE 550A (OH) anion exchange resin, leaving only stabilised Ag particles and NH_3 in solution.

Synthesis of Metal Nanoparticles for Nucleation and Growth Studies

Synthesis of metal particles was performed in a 50mL beaker with agitation provided using a magnetic stirrer. For the NaBH_4 reactions, the precursor metal ions were added to a solution containing the ammonium salt of the PEG-MA stabiliser. A ratio of metal ions to stabiliser carboxyl groups of 1 was used. The reaction mixture was brought to a volume of 15mL with deionised water. Mixing was initiated. 5mL of NaBH_4 solution was then added. 1 mol of NaBH_4 was used for every mol of electrons required to reduce the metal ions. A similar approach was adopted for the reactions in which hydrazine was used as a reductant. However, sufficient ammonia solution was also added to neutralise the by-product H^+ ions to prevent hydrazine decomposition. Hydrazine was then fed to the reactor via a Harvard Apparatus PHD2000 infusion pump.

Characterisation

Once the particulate solutions had been prepared they were characterised using a variety of techniques. Particles that were sufficiently small (generally less than 100nm in size) such that they could be maintained in suspension, were sized using a Malvern High Performance Particle Sizer (HPP5001). This instrument determines particle size through dynamic light scattering (DLS). Larger particles were sized using a Malvern Mastersizer 2000, which employs a laser diffraction technique to ascertain particle size.

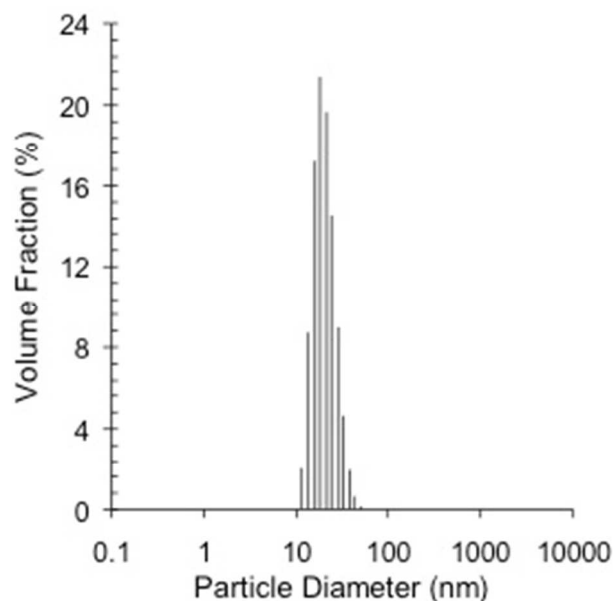
A FEI Tecnai F20 transmission electron microscopy (TEM) was used to confirm particles sizes and obtain information regarding the shape and structure of particles. Further analysis was conducted using a Cary 5 UV-vis spectrophotometer. This was used to confirm the formation of Ag and Au particles through

spectral absorption.

Results

Synthesis of Concentrated Ag Nanoparticles

Ag nanoparticles were successfully produced at concentrations up to 2.5mol/L. These colloidal suspensions were stable to further agglomeration for a period of months. Figure 1 shows the particle size distribution of the Ag nanoparticles. The particles had a



mean volume weighted diameter of 18nm with a standard deviation of 8nm.

Figure 1: Particle size distribution for Ag particles. Experimental conditions: $C_{\text{Ag}} = 2.5\text{mol/L}$, $\text{Ag}^+/\text{COO}^- = 10$, $t_{\text{feed}} = 2\text{hrs}$, $T = 293\text{K}$, and shear rate = 150s^{-1} .

Figure 2 shows TEM images of the Ag particles. The images highlight that the suspension is composed primarily of twinned Ag crystals with a mean diameter of around 15nm. There appears to be no agglomeration of particles. The TEM images confirm the particle size data derived from DLS.

The stabilised particles produced using this method can be dried down and fully redispersed in water. This suggests that the stabiliser is adsorbed very strongly to the particle surface. The particles exhibit excellent stability, with no aggregation, even after two years. The image in Figure 3 is of the dry silver nanoparticles and polymer mixture. It has a thick granulated gum like texture.

Figure 4 shows a UV-visible absorption spectrum of the particles in water. It is observed that there is a well defined plasmon band with a peak at a wavelength of 433nm, which is characteristic of Ag nanoparticle solutions⁵². There is no secondary shoulder present at higher wavelengths, indicating that agglomerate Ag nanoparticles have not formed in this system. Redispersion of the dried Ag particles results in the UV spectrum shown with the broken lines. The spectrum for the redispersed sample lies on top of the original spectrum, indicating that there is no aggregation of

particles during the drying and re-dissolution processes.

The experimental procedure, as described, was found to be the optimal method for synthesis of Ag nanoparticles using this system. Analysis of system parameters was conducted prior to high concentration synthesis. In particular the interaction between Ag^+ and the stabiliser, the optimal quantity of stabiliser required, and the source of the Ag^+ ions were assessed and are discussed later.

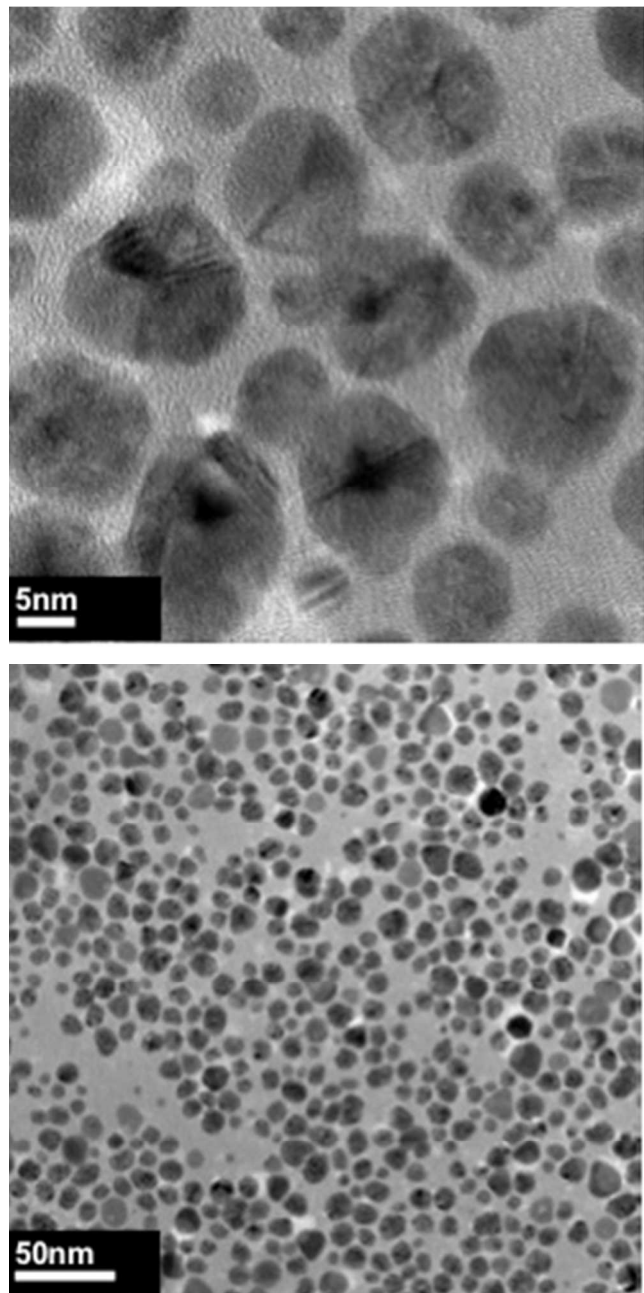


Figure 2: TEM images of Ag particles. Experimental conditions: $C_{\text{Ag}} = 2.5\text{mol/L}$, $\text{Ag}^+/\text{COO}^- = 10$, $t_{\text{feed}} = 2\text{hrs}$, $T = 293\text{K}$, and shear rate = 150s^{-1} .



Figure 3: Photograph of dried silver nanoparticle polymer composite.

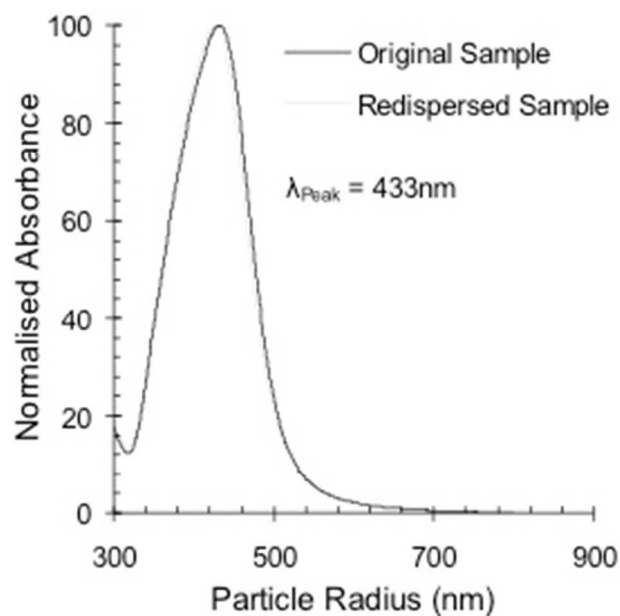


Figure 4: UV-vis absorption spectra for Ag particles. Drying and redissolving in water results in no change to the UV-vis spectra. Experimental conditions: $C_{\text{Ag}} = 2.5\text{mol/L}$, $\text{Ag}^+/\text{COO}^- = 10$, $t_{\text{feed}} = 2\text{hrs}$, $T = 293\text{K}$, and shear rate = 150s^{-1} .

Nucleation and Growth Studies of Metal Nanoparticles

Metal nanoparticles were formed using two modes of reduction from the precursor salt. These included: reduction of the metal ion with NaBH_4 , and reduction with hydrazine.

Figure 5 shows particle size data as a function of concentration for Ag, Au, Pd, and Pt reduced using NaBH_4 . The data indicates that at low concentrations, nucleation results in the formation of particles with an initial size of approximately 0.6nm. This is the smallest size that the DLS (Malvern HPP5001) can report. Au, Ag, Pd, and Pt all have an FCC structure, with an atomic packing factor of 0.74. Particles with a diameter of 0.6nm are calculated to contain approximately 7 atoms, based on an atomic radius of 0.144nm for Ag. These particles are thought to be the primary particles that have formed on nucleation.

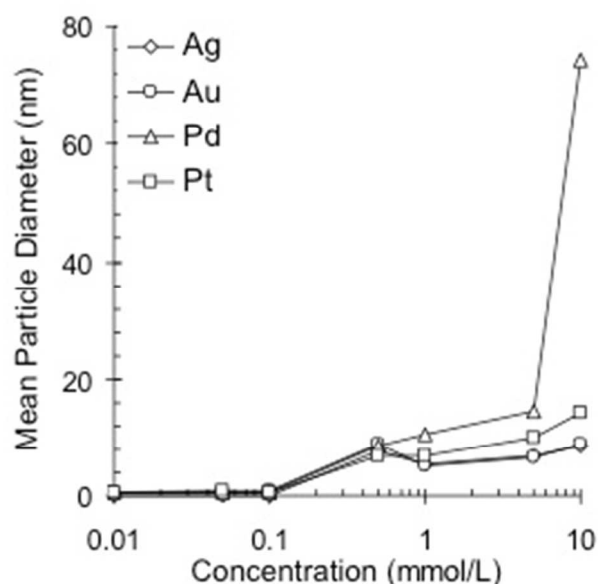


Figure 5: Particle Size vs. Concentration for Ag, Au, Pd, and Pt particles. Particles stabilised using PEG-MA at a metal ion/carboxyl group ratio of 2.

As the concentration of the suspension increases, there is an increase in final particle size. It is postulated that this size increase occurs as a result of the aggregation of primary particles. At higher concentrations the nucleation rate is more rapid, as higher concentrations favour nucleation over diffusive growth. An increase in the rate of nuclei generation is likely to result in aggregation due to an increase in the frequency of particle collisions. This allows less time for stabiliser adsorption to prevent the onset of aggregation. TEM images, for Ag and Pd systems, shown in Figure 6, confirm the sizing observations and furthermore suggest that there are different aggregative growth mechanisms present.

At low concentrations, the TEM images show very small spherical single crystal particles, with diameters <1nm. At moderate concentrations a combination of larger single crystal particles, with a size of around 5nm, and twinned particles, with a

size >10nm, are shown. It is thought that these larger single crystal particles have formed through aggregation of the small primary particles, with further aggregation resulting in the formation of the twinned particles. Further increasing the concentration results in a suspension primarily composed of polygonal twinned particles with regard to Ag and Au, or agglomerated particles in the case of Pd and Pt. The TEM images support the postulate that aggregative growth is dominant. Further work on particle size control in a range of systems is reported elsewhere^{53, 54}.

Figure 7 shows particle size data as a function of concentration for Ag and Pd produced using hydrazine. Experiments were conducted for Ag, Au, Pd and Pt. TEM images for Ag are reported in Figure 8. The results for Au were very similar to those obtained for Pd. Pt nanoparticles were unable to be formed using this method due to extensive particle aggregation.

It was observed during the synthesis of Ag nanoparticles that there is an induction period, during which no observable reduction reaction occurs. The induction period provides an opportunity for the quantitative evaluation of the nucleation and growth process. In order to assess the temporal evolution of Ag particles, a synthetic reaction was conducted in situ within a DLS instrument. It has previously been shown that the count rate and particle size data obtained in this manner from DLS, is in good agreement with similar data obtained using UV-vis spectroscopy⁵⁵.

A Ag particle synthesis experiment was conducted at a concentration of 5mmol/L. Figure 9 shows that there is an induction period of approximately 7 minutes, at this point a single nucleation event occurs and continues for approximately 5 minutes, a similar induction period was observed at concentrations of 10, 20, 50 and 100mmol/L. Furthermore, Figure 9 shows that the Ag particles that are generated at 5mmol/L form at a size of less than 1nm.

The presence of an induction period suggests that there is a strong interaction between the Ag^+ ions and the PEG-MA stabiliser. This induction period was not observed with any of the other systems. This may be as a result of Au, Pd, and Pt being reduced from a precursor anion. As such, it is expected that interaction with the carboxyl groups, for these metals, would result in electrostatic repulsion rather than strong coordination.

The induction period observed with Ag, allows homogenisation of the reaction medium prior to nucleation. This is favourable as it ensures that the nucleation events are spread throughout the total reaction volume. For the Au, Pd, and Pt systems, nucleation is observed to occur immediately upon the reductant being injected into the system. This results in a localised and highly concentrated nuclei population.

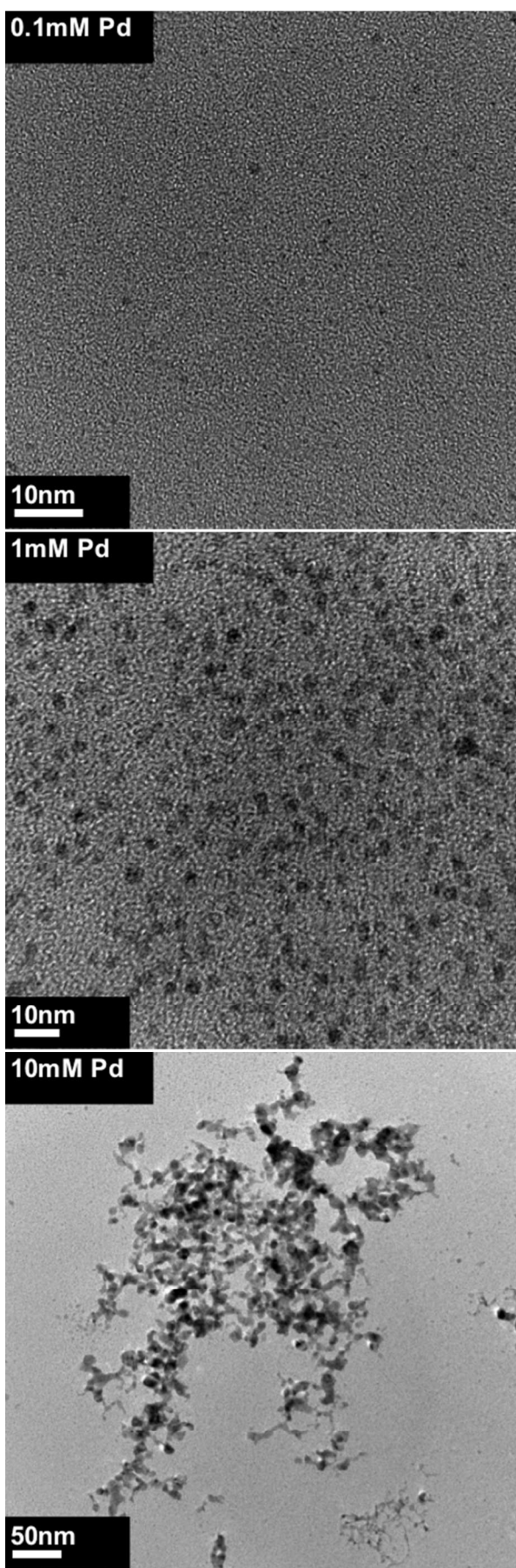
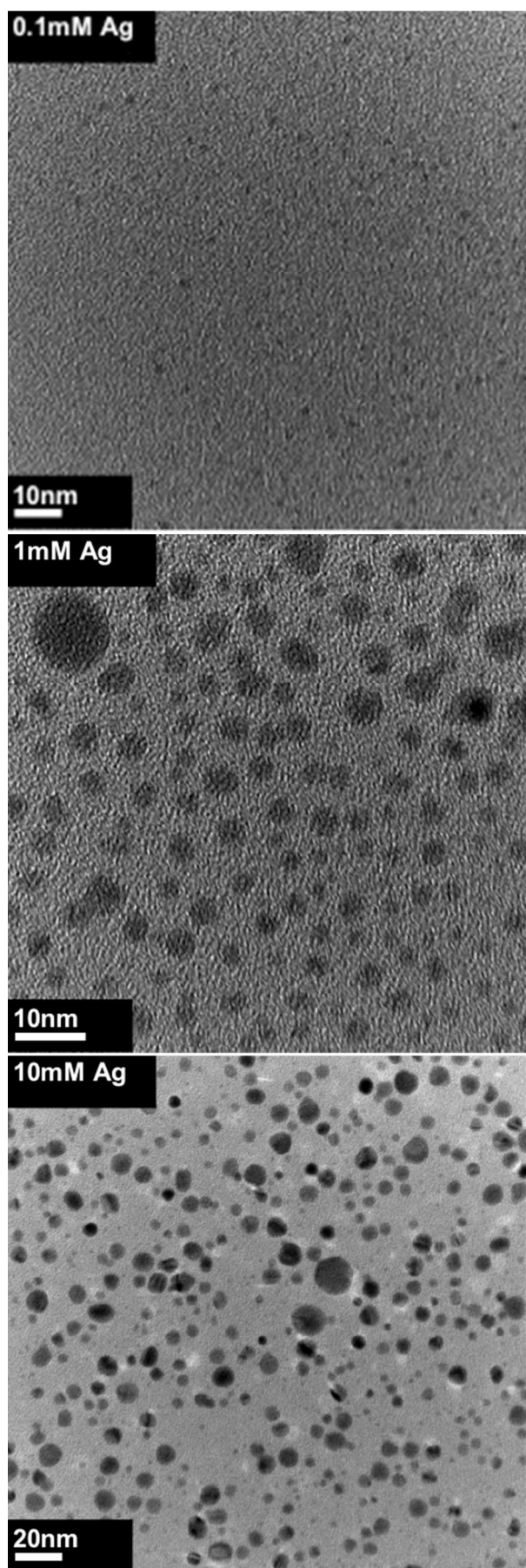


Figure 6: TEM images of Ag and Pd particles produced at 0.1, 1, and 10mmol/L.

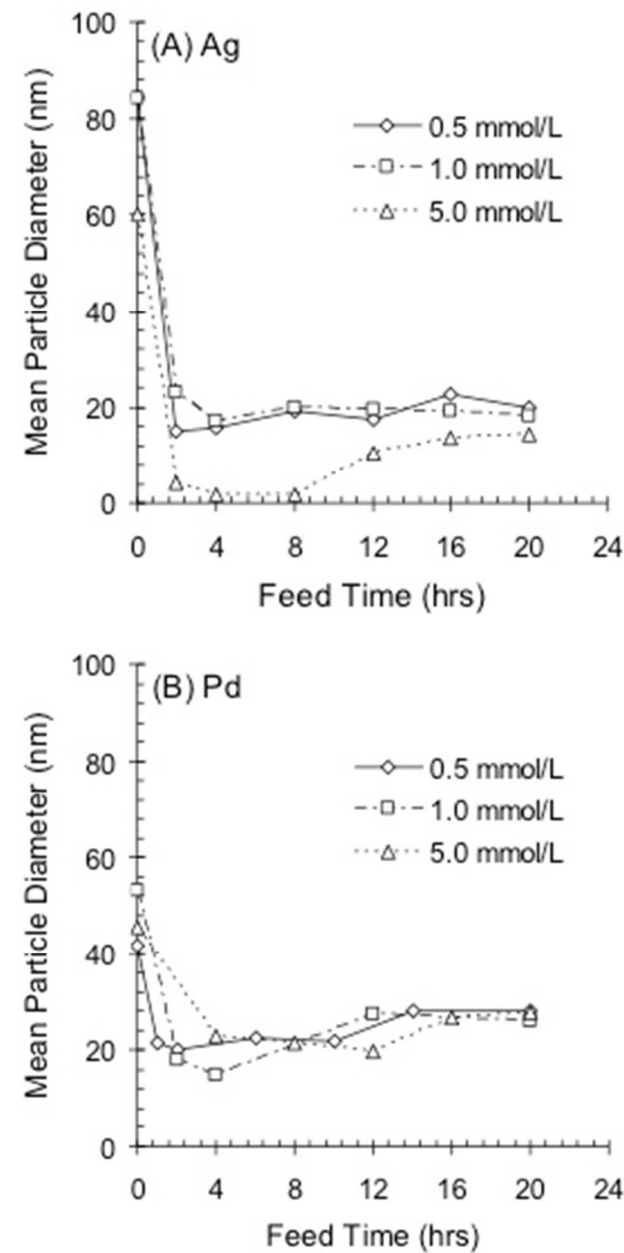


Figure 7: Mean particle diameter for experiments conducted at different feed times for: (A) Ag and (B) Pd. Particles were stabilised using PEG-MA at a metal ion/carboxyl group ratio of 2.

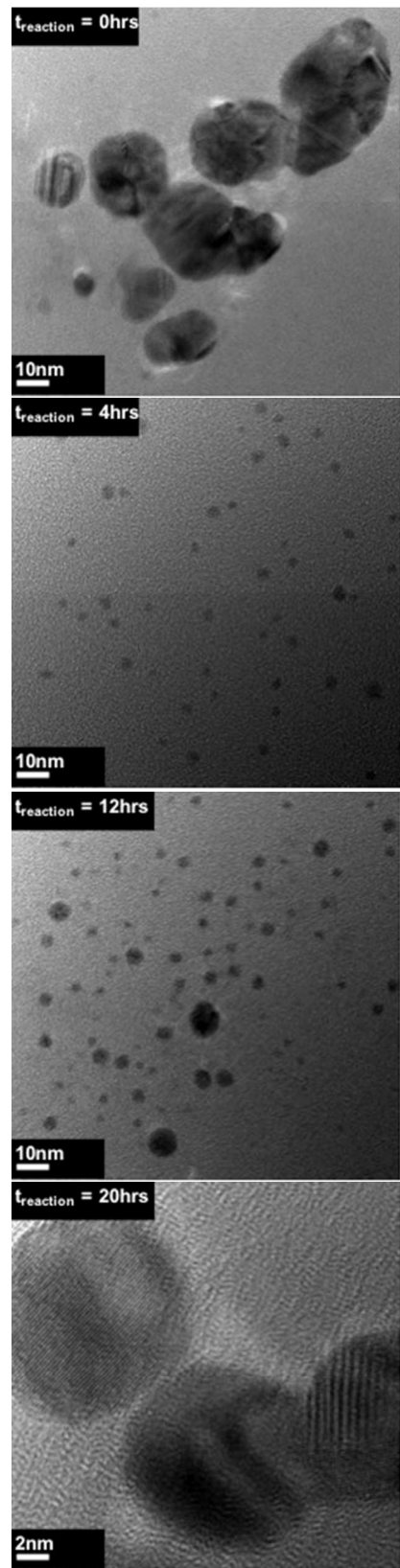


Figure 8: TEM images of PEG-MA stabilised Ag particles for experiments conducted at varying hydrazine feed rates.

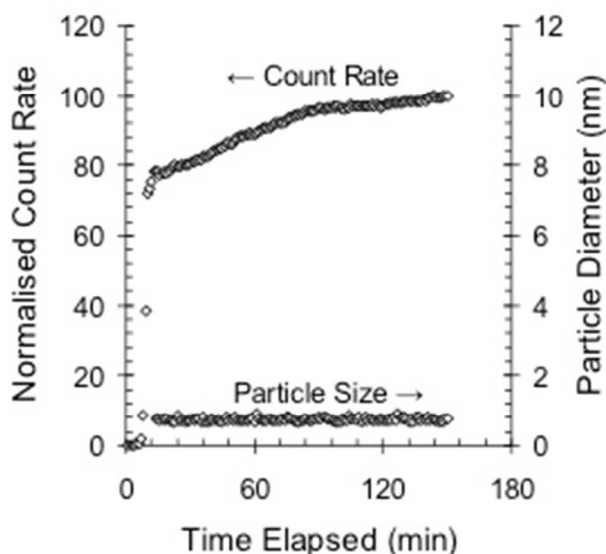


Figure 9: Relative Ag Particle Concentration and Median Ag Particle Size vs. Time. Experimental conditions: $C_{Ag} = 5\text{mmol/L}$, $Ag^+/COO^- = 2$, and $T = 298\text{K}$.

Discussion

There is significant interest in the synthesis of colloiddally stable and highly concentrated Ag nanoparticles. Ag nanoparticles possess unique optical properties, antimicrobial properties⁵⁶⁻⁵⁸, and have applications in biology⁵⁹, surface enhanced Raman spectroscopy⁶⁰⁻⁶², as catalysts, and in printed electronics^{5, 63-65}.

Many research groups have successfully synthesised Ag nanoparticle dispersions. However, many of these have been under very dilute conditions for the purpose of investigating distinct properties or interactions of Ag particles at a specific size such as: crystal growth^{34, 61, 66}, new routes for Ag synthesis⁶⁷⁻⁶⁹, or the impact of various stabilisers on Ag particle systems^{17, 19, 22, 24, 31}. In many of these instances, the synthetic route yields particles that are stable under relatively dilute conditions.

There are limitations with the current research in terms of being able to synthesise highly concentrated dispersions. A literature review yielded only a few research articles with a focus on producing concentrated Ag dispersions^{5, 30, 70}. Lee *et al.* produced Ag particles at 2mol/L in an organic solvent⁵. However, only one article was identified where reproducible and highly concentrated Ag nanoparticles were synthesised in water. Sondi *et al.* were able to produce Ag particles with a mean size of $26.3\text{nm} \pm 7.4\text{nm}$ in aqueous solution at 0.3mol/L using Daxad19 as the stabiliser³⁰. Daxad 19 consists of the sodium salt of polymerised alkylnaphthalene sulphonic acid.

There is a reported instance of the aqueous phase synthesis of Ag at a higher concentration. Ryu *et al.* claim to have produced particles in aqueous solution at 40wt% Ag, stabilised using polyacrylic ammonium salts (PAA) with $M_w = 1200 - 30,000$ ⁷⁰. It is unlikely that such a concentrated suspension of Ag particles could be produced using only PAA as the stabiliser. Although PAA has a backbone consisting of carboxyl groups, which are

known to have good affinity for the Ag surface, it possesses no dedicated steric component. Literature suggests that a dedicated steric component is important for the formation of stable suspensions at high concentrations.

Experiments were conducted to validate the results of Ryu *et al.* at 1wt% Ag. These experiments were unsuccessful and resulted in the formation of a Ag sediment phase. It was noted in some instances that dilution of the sediment resulted in a solution typical of Ag nanoparticles. This suggested that the adsorption was sufficiently strong as to prevent stabiliser displacement during particle coalescence, but the stabiliser was unable to maintain a minimum inter-particle distance to prevent flocculation due to van der Waals attraction. If the spectator ion species were removed, it is possible that electrostatic repulsion may overcome the Van der Waals attraction that caused flocculation. However, at the reaction concentration specified by Ryu *et al.*⁷⁰, electrostatic stabilisation would be negligible and attractive forces would dominate. As such, it is apparent that this method does not offer a reliable or easily reproducible synthetic route for the aqueous synthesis of Ag nanoparticles at high concentration.

It has been demonstrated that a PEG-MA comb polymer can be used to facilitate the synthesis and stabilisation of concentrated Ag nanoparticles. Further to this, a number of considerations for optimising the synthetic procedure were identified.

Pre-coordination of the Ag^+ with the carboxyl groups aligning the PEG-MA backbone was found to be important for reducing the potential for aggregation, and necessary for the formation of a viable nanoparticle suspension at high concentrations. Experiments were conducted looking at two other feed schemes. These were: (A) feeding $AgNO_3$ into a reaction vessel containing a PEG-MA and hydrazine NH_3 buffered solution, and (B) feeding both $AgNO_3$ and hydrazine through separate feeds into a solution containing PEG-MA and NH_3 buffered solution. In both of these cases there was no pre-coordination of Ag^+ with the carboxyl groups, and in both cases aggregation was observed.

Electrostatic attraction between the Ag^+ and the carboxyl groups is postulated to shorten the distance that the stabiliser must diffuse to reach the particle surface. This reduces the time it takes for particles to become stabilised, reducing the extent of aggregative growth mechanisms prior to stabiliser adsorption.

Furthermore, it was found that a ratio of Ag^+/COO^- of approximately 10 was necessary to ensure the formation of stable particles. This ratio corresponds to that required for full surface coverage at a mean particle size of 18nm. At ratios greater than this value, there was insufficient polymer for full surface coverage, and aggregation (into large micron sized particles) was observed. Excess polymer appeared to have no significant impact on reducing particle size.

The synthesis reaction was found to be insensitive to the silver precursor compound. Synthesis was conducted with $AgCH_3COO$, $AgClO_3$, and $AgClO_4$ at concentrations of 100mmol/L. No difference was observed in the particle size distributions in comparison to that obtained when using $AgNO_3$. In particular, it was thought that the carboxyl group present on the acetate anion may interfere and hinder the PEG-MA comb polymer adsorbing to the particle surface. Experiments were conducted with $AgCH_3COO$ at concentrations of up to 1mol/L with no

observable difference in particle size as compared with reduction of AgNO_3 . The synthetic procedure appears robust and insensitive to the presence of spectator ions.

After successful application of the PEG-MA molecule to the synthesis of concentrated Ag dispersions, an examination of the nucleation and growth processes of a range of metal nanoparticles was conducted in the presence of the PEG-MA stabiliser. Particles were produced via reduction with both NaBH_4 and hydrazine.

NaBH_4 is a potent reducing reagent that should ensure rapid reduction, and thus favours nucleation of particles⁵¹. This should allow assessment at low reactant concentrations, of the primary particle size and the primary method of particle growth under rapid nucleation conditions. Hydrazine is less reactive than NaBH_4 , and therefore a lower rate of nucleation would be expected. Hydrazine is therefore a more suitable reducing agent for use at high concentrations. Use of hydrazine may also allow examination of whether any diffusive growth is occurring, particularly if the nucleation rate is reduced by slowing the feed rate of hydrazine into the system.

It is postulated, particularly at higher concentrations, that the primary mode of growth is through aggregation. In order to examine the initial formation mechanisms, a range of experiments were conducted synthesising Au, Ag, Pd and Pt nanoparticles. These particles were produced over a range of concentrations from 0.01mmol/L to 10mmol/L. Particles were stabilised with a PEG-MA stabiliser. NaBH_4 was used as the reductant. The NaBH_4 was fed into the system in a single event. This was done so that only a single nucleation event occurred. In addition to providing a rapid reaction rate, NaBH_4 was also used due to the propensity of borohydride and borate anions to associate with metal particle surfaces providing a rapid and significant transient electrostatic barrier against aggregation^{28, 71}.

It was expected that at a sufficiently low concentration the transient electrostatic barrier offered by the borate and borohydride anions would allow sufficient time for stabiliser adsorption prior to particle aggregation. The rapid reduction rate should prevent or limit diffusive growth processes. In the absence of aggregation and diffusive growth, the particles should form at the critical size predicted by the Gibbs-Thomson Equation:

$$r^* = 2\gamma V_M / RT \ln S \quad (2)$$

Where r^* is the critical radius, γ is the surface energy, V_M is the molar volume, R is the gas constant, T is the absolute temperature, and S is the degree of supersaturation.

Figure 10 shows the critical radius of silver particles as a function of supersaturation according to the Gibbs-Thomson Equation. The surface energy for a silver particle has been approximated as 120mJ/m²⁷².

Metals are highly insoluble and so even at low concentrations the degree of supersaturation is very high. The critical radius for Ag decreases rapidly with an increase in the supersaturation level. At a supersaturation value of 300, the critical radius of an Ag particle becomes equivalent to the atomic radius of silver (0.144nm). The atomic radius represents the size of a single atom, and therefore the minimum physical size possible. Similarly, it is expected that at a supersaturation rate of 300, the nucleation rate

will approach the maximum rate possible for these systems (i.e. $J_N = J_0$).

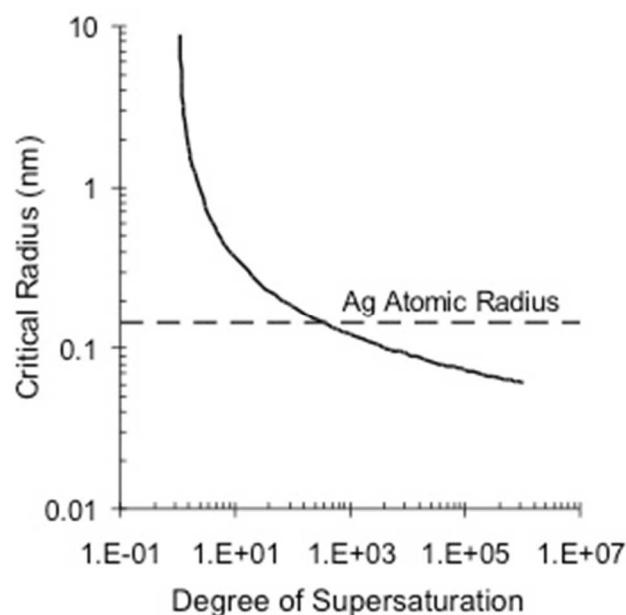


Figure 10: The critical radius of Ag particles as a function of the degree of supersaturation. Broken horizontal line represents atomic radius of a silver atom.

The largest particles formed, and thus the system that exhibits the highest degree of aggregation as the concentration is increased, is the Pd system, followed by Pt, then Au, and finally Ag. This is the same order as the galvanic series. The galvanic series relates the nobility or preference of a metal to exist in its elemental state when in an ionic solution. It is likely that the reaction rate follows this order. Therefore, it is expected that materials higher in the galvanic series exhibit a higher nucleation rate. This would result in more extensive aggregation prior to stabiliser adsorption. This reactivity order is not representative of that for diffusional growth, and so is different to the order proposed by Finney and Finke⁷³ from the studies conducted by Bönneman *et al.*⁷⁴ and Hirai *et al.*⁷⁵.

Based on the results of Figures 5 and 6, the growth mechanism shown in Figure 11 is proposed. The mechanism is aggregative in nature. Stabiliser adsorption can arrest the aggregative process at any stage, preventing further increase in particle size due to aggregation.

Upon addition of the NaBH_4 to the system, nucleation occurs resulting in the formation of primary particles, of approximate size 0.6nm, shown at stage (A).

At stage (B) aggregation of the primary particles occurs. The TEM images show that these secondary particles are generally devoid of multiple planes and possess a coherent crystal structure, as shown at stage (C). This suggests that aggregation of the primary particles occurs along high energy interfaces with dissolution of any potential grain boundaries and full co-integration of the primary particles into typical nanoparticles. These secondary particles have a diameter that is of the order of 5nm.

At stage (D) aggregation of the secondary particles occurs through a twinning mechanism (E). These twinned particles still have the appearance of discrete particles, but have taken on a polygonal shape due to the presence of discernable twinned planes, shown at stage (F). Further aggregation results in agglomerate particles that consist of multiple adjoining particles.

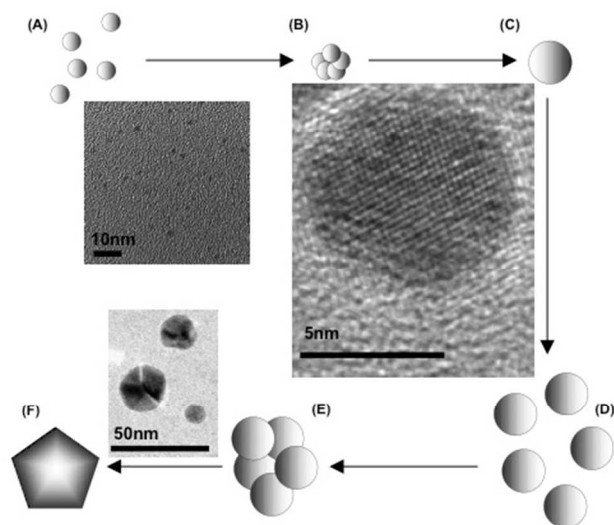


Figure 11: Proposed aggregative growth mechanism.

In systems that exhibit a high nucleation rate, there will be a higher nuclei density and a shorter mean distance between nuclei. As a consequence, the stabilising molecule has less time to adsorb and provide stability than in a system with fewer more distant nuclei. If the stabiliser is unable to adsorb rapidly, aggregation of the primary particles into secondary particles occurs. The effectiveness of a stabiliser is dependent on both the rate and strength of adsorption. NaBH_4 is highly reactive, and its use results in the rapid reduction of metal ions. It was found to be unsuitable for use in the highly concentrated synthesis of nanoparticles in aqueous PEG-MA systems. Hydrazine is a reductant that is also used in the synthesis of metal nanoparticles. It is less reactive than NaBH_4 and thus provides a lower reaction rate. This potentially lowers the initial rate of aggregation, and possibly allows an opportunity for diffusive growth processes to occur.

Experiments were conducted with the aim of determining the effect of hydrazine feed rate on the formation of a viable particle suspension. As with the NaBH_4 system, it was expected that high feed rates should favour the formation of small particles. This is because the simultaneous presence of a high concentration of reactants favours the rapid formation of many small nuclei. Continuous nucleation would be expected with minimal diffusive growth. However, at a reduced feed rate, the quantity of hydrazine in the system at any given time would be lower. As a result, the motivation for nucleation would be reduced, while that for diffusive growth would be increased. With a sufficiently low feed rate, growth through monomeric diffusion would potentially be favoured at the expense of continuous nucleation. This is because homogenous nucleation has a higher activation energy

than that required for diffusive growth^{76, 77}. This may potentially provide a means for controlling the particle size, allowing control of the desired mean size through tuning of the particle growth rate.

Figure 7 indicates that aggregative growth occurred in all instances prior to stabiliser adsorption. Particles formed in the experiment with addition of an immediate stoichiometric quantity of hydrazine (feed time = 0) provides a direct comparison with the NaBH_4 reduced metal samples. Although the rate of reaction is lowered when using hydrazine as the reductant, larger particles are formed than with NaBH_4 . This suggests that in the absence of the initial electrostatic barrier provided by the adsorption of borate and borohydride anions at the particle surface, the aggregation posed by the simultaneous presence of excess nuclei prior to stabiliser adsorption is not mitigated by the decreased nucleation rate.

As the reaction time is increased, the response at short reaction times is an initial decrease in particle size. This is postulated to occur as the rate of nuclei formation is reduced due to multiple nucleation events spread out over time. This lowers the nuclei population at any given moment and as such, the mean distance between nuclei is greater, allowing time for the stabiliser to adsorb and stabilise the particles without the level of aggregation observed in the instantaneous feed experiments.

Increasing the reaction time, typically beyond 4 hours, results in an increase in the mean particle size. This trend is particularly apparent for Ag particles produced at 5mM. It is postulated that the subsequent increase in particle size is due to diffusive growth. As the feed time is increased, the nucleation rate is lowered. This reduces the chance for aggregation prior to polymer adsorption. In a system in which no diffusive growth can occur, and the only growth mechanism is through aggregation, there will be a minimum particle size. This particle size will be dependent on the nucleation rate and degree of aggregation possible on the addition of a single drop of reductant. Further increasing the feed rate would have no effect on decreasing the particle size. Therefore, the observed increase in particle size with increasing feed rate is likely as a result of diffusive growth.

As the concentration increases, there appears to be an overall reduction in the mean particle size. It is thought that the lower concentration reactions favour diffusive growth. This may contribute to the larger particle sizes observed.

The 5mmol/L Ag series of experiments provide an example of the feed time exhibiting control over the final mean particle size. The particle size data of Figure 7, shown as TEM images in Figure 8, indicated that on instantaneous mixing of the reductant, typical agglomerate particles are produced. However, as the feed time is increased and the reaction time is slowed, small single crystal particles with a mean diameter of around 2nm are produced. This synthetic process is robust with experiments ranging from 2hrs to 8hrs in duration producing similar results. Increasing the experiment time beyond 8hrs resulted in an increase in the mean particle size. Many of the larger particles (around 14nm in diameter) that formed in the experiment with the 20hr reaction time appear to be single crystal particles expressing a single crystal plane. The particles appear to have grown through a diffusive process rather than aggregation, twinning or agglomeration. This suggests that by controlling the feed rate,

either nucleation or growth can be encouraged. This potentially allows the final mean particle size to be controlled.

Pd and Au particles all grew through an initial aggregation phase prior to adsorption of the PEG-MA stabiliser. This is attributed primarily to the higher nucleation rates exhibited by these metals over that of Ag. However, another contributing factor is that both Au and Pd are reduced from a precursor anion. The carboxyl groups on the polymer backbone and the $\text{PdCl}_6^{2-}/\text{AuCl}_4^-$ have a like charge, so electrostatic repulsion will occur. Attraction will not occur until the anion has been reduced to the metal. As a result there will be no close association of the precursor reagents and the stabiliser, as is postulated with Ag (which is reduced from a cation). The stabiliser will take an increased amount of time to adsorb to the Au or Pd surface as it was not closely associated with the precursor ion prior to reduction. This increased time to stabilisation is thought to facilitate aggregation of primary and secondary particles.

Conclusions

A PEG-MA copolymer has been used successfully to facilitate synthesis of highly concentrated Ag suspensions in water. Ag particles with a mean diameter of 18nm were synthesised at a maximum concentration of 2.5mol/L at a $\text{Ag}^+:\text{COO}^-$ ratio of 10. The Ag solution can be fully dried and redispersed in water without any loss in particle dispersion quality. Sufficient stabiliser is required to ensure that full surface coverage of particles occurs.

Coordination of Ag^+ with the COO^- groups on the stabiliser was found to be important. The electrostatic attraction between the Ag^+ and the carboxyl groups is postulated to shorten the distance that the stabiliser must diffuse to reach the particle surface. This reduces the time it takes for particles to become stabilised, limiting the extent of aggregation prior to stabiliser adsorption. The formation mechanism of metal nanoparticles under concentrated conditions in an aqueous environment has been evaluated for Ag, Au, Pt and Pd. The results suggest that the formation mechanism is primarily aggregative in nature. Small particles that are around 0.6nm in size are initially formed; these particles are estimated to contain around 7 atoms. Larger single crystal metal particles with a diameter of approximately 5nm are formed via aggregation of these primary particles. In many systems, the grain boundaries that distinguish the original nuclei are thought to undergo dissolution as a result of diffusive processes. Further aggregation results in polygonal twinned particles. If aggregation continues beyond this point, agglomerate particles are formed. The role of the co-polymer in imparting dispersion stability is observed to be critical to particle size control by preventing further aggregation. This mechanism appears to be generic under concentrated synthesis conditions.

Acknowledgements

The financial support of this work through the ICI Strategic Research Fund and infrastructure support through the Particulate and Fluids Processing Centre, a Special Research Centre of the Australian Research Council is gratefully acknowledged.

References

1. J. P. Holdren, *National Nanotechnology Initiative - Supplement to the President's 2010 Budget*, Washington D.C., 2009.
2. S. Deki, H. Yanagimoto, S. Hiraoka, K. Akamatsu and K. Gotoh, *Chemistry of Materials*, 2003, **15**, 4916-4922.
3. T. Gacoin, L. Malier, G. Cournio and J.-P. Boilot, *Proceedings of SPIE - The International Society for Optical Engineering*, San Diego, CA, United States, 1997.
4. M. Iijima, K. Sato, K. Kurashima, T. Ishigaki and H. Kamiya, *Powder Technology*, 2008, **181**, 45-50.
5. K. J. Lee, B. H. Jun, T. H. Kim and J. Joung, *Nanotechnology*, 2006, **17**, 2424-2428.
6. Y. Li, X. Li, C. Yang and Y. Li, *Journal of Materials Chemistry*, 2003, **13**, 2641-2648.
7. A. Nanni and L. Dei, *Langmuir*, 2003, **19**, 933-938.
8. I.-K. Shim, Y. I. Lee, K. J. Lee and J. Joung, *Materials Chemistry and Physics*, 2008, **110**, 316-321.
9. H. Shimooka, T. Tanizaki, M. Mitome, Y. Bando and S. Kohiki, *Journal of Crystal Growth*, 2005, **275**, e2377-e2381.
10. S.-H. Wu and D.-H. Chen, *J. Coll. Int. Sci.*, 2004, **273**, 165-169.
11. A. A. Athawale, S. V. Bhagwat, P. P. Katre, A. J. Chandwadkar and P. Karandikar, *Materials Letters*, 2003, **57**, 3889-3894.
12. M. Brust and C. J. Kiely, *Colloids and Surfaces A: Physicochemical and Engineering Aspects*, 2002, **202**, 175-186.
13. M. Chen, P. T. Elliott and J. E. Glass, *Colloids and Surfaces A: Physicochemical and Engineering Aspects*, 2001, **183-185**, 457-474.
14. D.-W. Deng, J.-S. Yu and Y. Pan, *J. Coll. Int. Sci.*, 2006, **299**, 225-232.
15. K. Ishizu, H. Kakinuma, K. Ochi, S. Uchida and M. Hayashi, *Polymers for Advanced Technologies*, 2005, **16**, 834-839.
16. M. Kucher, D. Babic and M. Kind, *Chemical Engineering and Processing*, 2006, **45**, 900-907.
17. G. Li, Y. Luo and H. Tan, *Journal of Solid State Chemistry*, 2005, **178**, 1038-1043.
18. M. Li, Hari-Bala, X. Lv, X. Ma, F. Sun, L. Tang and Z. Wang, *Materials Letters*, 2007, **61**, 690-693.
19. C. Luo, Y. Zhang, X. Zeng, Y. Zeng and Y. Wang, *J. Coll. Int. Sci.*, 2005, **288**, 444-448.
20. G. A. Martinez-Castanon, M. G. Sanchez-Loredo, H. J. Dorantes, J. R. Martinez-Mendoza, G. Ortega-Zarosa and F. Ruiz, *Materials Letters*, 2005, **59**, 529-534.
21. P. Mulvaney, *Colloids and Surfaces A: Physicochemical and Engineering Aspects*, 1993, **81**, 231-238.
22. R. Pataklalvi, Z. Viranyi and I. Dekany, *Colloid & Polymer Science*, 2004, **283**, 299-305.
23. A. Petrova, W. Hintz and J. Tomas, *Chemical Engineering and Technology*, 2008, **31**, 604-608.
24. D. Radziuk, A. Skirtach, G. Sukhorukov, D. Shchukin and H. Mohwald, *Macromolecular Rapid Communications*, 2007, **28**, 848-855.
25. P. Rodriguez, N. Munoz-Aguirre, E. San-Martin Martinez, G. Gonzalez de la Cruz, S. A. Tomas and O. Zelaya Angel, *Journal of Crystal Growth*, 2008, **310**, 160-164.
26. T. Sakai and P. Alexandridis, *Langmuir*, 2004, **20**, 8426-8430.
27. T. Sakai and P. Alexandridis, *Journal of Physical Chemistry B*, 2005, **109**, 7766-7777.
28. Y.-S. Shon and E. Cutler, *Langmuir*, 2004, **20**, 6626-6630.
29. S. N. Sidorov, L. M. Bronstein, P. M. Valetsky, J. Hartmann, H. Colfen, H. Schnablegger and M. Antonietti, *J. Coll. Int. Sci.*, 1999, **212**, 197-211.
30. I. Sondi, D. V. Goia and E. Matijevic, *J. Coll. Int. Sci.*, 2003, **260**, 75-81.
31. Y. Tan, Y. Li and D. Zhu, *J. Coll. Int. Sci.*, 2003, **258**, 244-251.
32. A. V. Vivek, S. M. Pradipta and R. Dhamodharan, *Macromolecular Rapid Communications*, 2008, **29**, 737-742.

33. S. Wan, J. Huang, H. Yan and K. Liu, *Journal of Materials Chemistry*, 2005, 298-303.
34. D. Wang, C. Song, Z. Hu and X. Zhou, *Materials Letters*, 2005, **59**, 1760-1763.
35. Z. Wang, B. Tan, I. Hussain, N. Schaeffer, M. F. Wyatt, M. Brust and A. I. Cooper, *Langmuir*, 2007, **23**, 885-895.
36. D. C. Y. Wong, Z. Jaworski and A. W. Nienow, *Chemical Engineering Science*, 2001, **56**, 727-734.
37. Y. Liu, S. Z. D. Cheng, X. Wen and J. Hu, *Langmuir*, 2002, **18**, 10500-10502.
38. K. Shirahama, K. Nakao, H. Endo and R. Matuura, *Bulletin of the Chemical Society of Japan*, 1966, **39**, 1017-1019.
39. P. Somasundaran and L. Huang, *Advances in Colloid and Interface Science*, 2000, **88**, 179-208.
40. D. H. Napper, *J. Coll. Int. Sci.*, 1977, **58**, 390-407.
41. A. B. R. Mayer, *Polymers for Advanced Technologies*, 2001, **12**, 96-106.
42. D. H. Napper, *Polymeric Stabilization of Colloidal Dispersions*, Academic Press Inc. Ltd., London, 1983.
43. P. F. Luckham, *Advances in Colloid and Interface Science*, 2004, **111**, 29-47.
44. B. A. Rozenberg and R. Tenne, *Progress in Polymer Science*, 2008, **33**, 40-112.
45. T. Corner and R. Buscall, *US4460732*, 1984.
46. R. Buscall and T. Corner, *EP99179*, 1987.
47. R. Buscall, P. J. Scales, S. J. Williams and J. E. Newton, *EP395243*, 1989.
48. R. Buscall and S. J. Williams, *EP398487*, 1989.
49. S. J. Williams and R. Buscall, *US5084502*, 1992.
50. F. A. Holland and F. S. Chapman, *Liquid mixing and processing in stirred tanks*, Reinhold Publishing Corporation, New York, 1966.
51. D. V. Goia and E. Matijevic, *New Journal of Chemistry*, 1998, **Vol 22**, 1203 - 1215.
52. K.-C. Lee, S.-J. Lin, C.-H. Lin, C.-S. Tsai and Y.-J. Lu, *Surface and Coatings Technology*, 2008, **202**, 5339-5342.
53. R. Buscall, R. Graham, R. Anderson, P. J. Scales, P. Mulvaney and R. Eldridge, *EP2009067014*, 2009.
54. R. Buscall, R. Graham, R. Anderson, P. J. Scales, P. Mulvaney and R. Eldridge, *EP2009067015*, 2009.
55. L. D'Souza, A. Suchopar and R. M. Richards, *J. Coll. Int. Sci.*, 2004, **279**, 458-463.
56. S. Agnihotri, S. Mukherji and S. Mukherji, *Nanoscale*, 2013, **5**, 7328-7340.
57. V. D'Britto, H. Kapse, H. Babrekar, A. A. Prabhune, S. V. Bhoraskar, V. Premnath and B. L. V. Prasad, *Nanoscale*, 2011, **3**, 2957-2963.
58. A. Panacek, L. Kvitek, R. Prucek, M. Kolar, R. Vecerova, N. Pizurova, V. K. Sharma, T. Nevecna and R. Zboril, *Journal of Physical Chemistry B*, 2006, **110**, 16248-16253.
59. R. C. Doty, T. R. Tshikhudo, M. Brust and D. G. Fernig, *Chem. Mater.*, 2005, **17**, 4630-4635.
60. P. C. Andersen, M. L. Jacobson and K. L. Rowlen, *Journal of Physical Chemistry B*, 2004, **108**, 2148-2153.
61. L. Lu, A. Kobayashi, K. Tawa and Y. Ozaki, *Chemistry of Materials*, 2006, **18**, 4894-4901.
62. X. Zou and S. Dong, *Journal of Physical Chemistry B*, 2006, **110**, 21545-21550.
63. B. T. Nguyen, J. E. Gautrot, M. T. Nguyen and X. X. Zhu, 2007 NSTI Nanotechnology Conference and Trade Show - NSTI Nanotech 2007, May 20-24 2007, Santa Clara, CA, United States, 2007.
64. A. Kamyshny, M. Ben-Moshe, S. Aviezer and S. Magdassi, *Macromolecular Rapid Communications*, 2005, **26**, 281-288.
65. S. Gamerith, A. Klug, H. Scheiber, U. Scherf, E. Moderegger and E. J. W. List, *Advanced Functional Materials*, 2007, **17**, 3111-3118.
66. D. L. Van Hying, W. G. Klemperer and C. F. Zukoski, *Langmuir*, 2001, **17**, 3128-3135.
67. A. Manna, T. Imae, M. Iida and N. Hisamatsu, *Langmuir*, 2001, **17**, 6000-6004.
68. D. D. Evanoff and G. Chumanov, *J. Phys. Chem. B*, 2004, **108**, 13948-13956.
- L. Suber and W. R. Plunkett, *Nanoscale*, 2010, **2**, 128-133.
- B.-H. Ryu, Y. Choi, H.-S. Park, J.-H. Byun, K. Kong, J.-O. Lee and H. Chang, *Colloids and Surfaces A: Physicochemical and Engineering Aspects*, 2005, **270-271**, 345-351.
- D. L. Van Hying and C. F. Zukoski, *Langmuir*, 1998, **14**, 7034-7046.
- H. L. Skriver and N. M. Rosengaard, *Physical Review B (Condensed Matter)*, 1992, **46**, 7157-7168.
- E. E. Finney and R. G. Finke, *J. Coll. Int. Sci.*, 2008, **317**, 351-374.
- H. Bönnemann, G. Braun, W. Brijoux, R. Brinkmann, A. S. Tilling, K. Seevogel and K. Siepen, *Journal of Organometallic Chemistry*, 1996, **520**, 143-162.
- H. Hirai, Y. Nakao and N. Toshima, *Journal of macromolecular science. Chemistry*, 1979, **A13**, 727-750.
- D. J. Safarik and C. B. Mullins, *J. Chem. Phys.*, 2004, **121**, 6003-6010.
- D. Xiao-qing, T. Jing-you, M. Chuan-min and Z. Min-guang, *Journal of Synthetic Crystals*, 2004, **33**, 118-122.